PANEL FLUTTER CONTROL AT HIGH SUPERSONIC SPEED USING PIEZOELECTRIC MATERIAL

التحكم فى رفرفة الألواح التى تعمل على سرعات تفوق سرعة الصوت بإستخدام مواد البيزوإلكتريك

ABOU-AMER S. A
Vice Dean of AHI for management & Informatics

الخلاصة

تتعرض الألواح الخارجية المكونة للكساء الخارجى للمركبات التى تطير بسرعات أعلى من سرعة الصوت فى الغلاف الخارجى لما يسمى بالإهتزازات المثارة ذاتيا من النوع ذو الترددات المحدودة. إن تطور الطرق المستخدمة فى التحكم فى هذه الظاهرة مطلوب وهو الهدف من هذه الدراسة.

وفى هذه الدراسة تم إستخدام المعادلات اللاخطية للألواح بموائمة كل من نظرية الإنحناءات الكبيرة فى الألواح لفان كارمن والنظرية الإيروديناميكية الخطية لسيال الهواء المنتظم دلى سطح الألواح لتتناسب الحالة تحت الدراسة وهى عبارة عن لوح من الديور ألومنيوم مثبت علية من كلا السطحين العلوى والسفلى مادة البيزوإليكتريك تثبيتا جيدا.

وعند تطبيق قدر مناسب من الفولت على مادة البيزوإليكتريك فإنه ينتج نوع من التمدد العرضى لمادة اللوح وبالتالى حدوث ما يسمى بقوى الشد والمؤثرة فى مستوى اللوح. وهذه القوى تؤثر تأثيرا إيجابيا بترحيل نقطة تعرض اللوح لظاهرة الرفرفة إلى قيمة أعلى من القيمة التى يعمل عندها اللوح بدون المعالجة التى أجريت عليه.

وفى هذه الدراسة تم إيضاح قيم فولت التحكم وكذلك خواص وتأثير مواد البيزوإلكتريك على الألواح من خلال مقارنة النتائج الخاصة بظاهرة الرفرفة للألواح بعد المعالجة وقبلها. وقد أثبتت النتائج فى هذه الدراسة بنجاح النموذج المقترح بالتحكم فى إيقاف ظاهرة الرفرفة للألواح فى ظروف عملها.

Abstract

Exterior panels forming the skin of flight vehicles traveling through the atmosphere at high supersonic speed are often susceptible to the occurrence of limit-cycle type self-excited vibrations called flutter. The development of methods for panel flutter control is desirable and it is the objective of this work by using piezoelectric materials.

The nonlinear equations of motion for panel flutter using Von-Karman's large deflection plate theory and the quasi-steady aerodynamic theory are modified to consider the composite plate with the piezoelectric layer. The composite plate consists of two piezoelectric layers bonded perfectly to the upper and lower surface of the original panel layer.

When a voltage is applied to the piezoelectric layers, an induced strain in the plate material take place and consequently tensile in-plane load is obtained. These tensile loads shift the onset of flutter point to about twice the value of the critical dynamic pressure for the plate alone.

The values of control voltage and the effect of piezoelectric material properties are investigated. The method gives good results and succeeds in suppressing the panel flutter at its operating condition.

KEY WORDS

I. Introduction:

Panel flutter results from the interaction between the panel and the flow pressure forces brought about by the panel motion. This causes a loss of the stability of the panel in its un-deformed shape, so that any disturbance applied to it leads to oscillations of growing amplitude. Thus, it is a self excited oscillation resulting from the dynamic instability of the aerodynamic, inertia, and elastic forces of the system. This growth is limited, however, by the membrane tension stresses induced in the panel by the flutter motion itself. The result of this self-limiting action is a sustained oscillation of constant amplitude, called limit-cycle motion.

Due to the complexity of panel flutter, most theoretical studies make use of simplified assumptions, see Ref [13]. However these assumptions are usually so restrictive that the theoretical model does not accurately represent realistic conditions. In fact it is found that the application of the exact aerodynamic theory does not remove the discrepancies that presently exist between theory and experiment for flutter of stressed panels. The inclusion of structural damping is found to have a large effect in some instances and can tend to eliminate some of the differences. Von Karman's large deflection plate theory and quasi-steady aerodynamic theory have been employed. Galerkin's technique has been used in the space variables and the ordinary differential system obtained is solved by method of describing functions/harmonic balance method or direct numerical integration. The results obtained show that, as a first approximation, the amplitude of the limit cycle depends only upon the fundamental parameter (non-dimensional aerodynamic loading), the aspect ratio, and the damping parameter (including structural damping effect). The results are in excellent agreement with those obtained numerically in Ref. [5].

Agreement between theory and experiment improves at the higher Mach numbers. The disagreements between theory and experiment are mainly due to four factors:

1- The use of linear aerodynamic theory, where most of the theoretical investigations have utilized two-dimension static aerodynamic theory (both with and without damping), despite the fact that two dimensional theory is considered applicable only for a limited range of panel length-to-width ratio and Mach number.

2- Neglecting boundary layer and aerodynamic heating effects.

3- The imprecise idealization of the complicated panel support conditions and cavity.

4- Neglecting nonlinear mid-plane stresses and buckling.

Considering all of the above factors in formulating the mathematical model, the results of the theory and the experiment will be in excellent agreement. Flutter oscillations rarely cause immediate failure of the panel, but they may produce fatigue failure after a sufficient period of time. The need to prevent this occurrence, either by suppressing flutter entirely or by limiting the severity of the panel motion, often becomes the critical design criterion that determines the required thickness (or more generally the stiffness) of the panel, see Ref [16]. Many parameters govern the resonance fatigue behavior including the detail design, the skin thickness and materials, the stiffener configurations and the damping of the structure. The new technology for flutter prevention is to use piezoelectric actuators to produce an induced strain and, consequently, in-plane tensile forces to stabilize the plate during flutter. The plate with the piezoelectric actuators and sensors are called controlled structures (or smart

structures), where both sensors and actuators are connected through a feedback loop, see Ref. [19] and [25]. There are two types of controlled structures called vibration control and shape control. Actually in vibration control, the objective is to change the dynamic properties of the structure, such as damping. To do this, relatively small forces can be exerted on many flexible modes by relatively small number of actuators. The most common form of vibration control entails the addition of active damping by the feedback of measured or inferred rate to actuators, see Ref [20]. The purpose of such active damping is to reduce the response of the structure. Another concept, closely related to active damping is active stabilization, in which initially unstable modes are stabilized by closed loop control see Ref. [23].

II. Problem Formulation

The plate under consideration with cavity is shown in Fig. 1 with dimension and properties shown in Table. 3. The axes are taken to be such that the x-, y-axes are in the plane of the plate passing through its reference plane (z=0), while the z- axis is positive upwards. Under the assumptions that plate thickness is small in comparison with smallest lateral dimension, which is the case in most practical applications, the Kirchhoff's hypothesis may be assumed to be valid. With this assumption the in-plane displacements "u", "v" and the transverse deflection "w" at an arbitrary point of the plate in the x, y, and z directions will be as given in Ref. [13] and [27]. The plate aero-elastic equations in a non-dimensional form are finally will be:

The U-equation is given as:

$$\overline{u}_{,\xi\xi}+d_1f^2\overline{u}_{,\eta\eta}+d_2f\overline{v}_{,\xi\eta}+\frac{h}{a}\{\overline{w}_{,\xi}\overline{w}_{,\xi\xi}+$$
$$d_1f^2\overline{w}_{,\xi}\overline{w}_{,\eta\eta}+d_2f^2\overline{w}_{,\eta}\overline{w}_{,\xi\eta}\}=0 \qquad (1\text{-}a)$$

The V-equation is given as:

$$d_1\overline{v}_{,\xi\xi}+f^2\overline{v}_{,\eta\eta}+d_2f\overline{u}_{,\xi\eta}+\frac{h}{b}\{f^2\overline{w}_{,\eta}\overline{w}_{,\eta\eta}+$$
$$d_1\overline{w}_{,\eta}\overline{w}_{,\xi\xi}+d_2\overline{w}_{,\xi}\overline{w}_{,\xi\eta}\}=0 \qquad (1\text{-}b)$$

The W-equation is given as:

$$\frac{1}{\pi^4}\{\overline{w}_{,\xi\xi\xi\xi}+2f^2\overline{w}_{,\xi\xi\eta\eta}+f^4\overline{w}_{,\eta\eta\eta\eta}\}\pm\{$$
$$\overline{n}_\eta{}^{(AL)}+\overline{n}_\eta{}^{(AT)}\}\pm\{\overline{n}_\xi{}^{(AL)}+\overline{n}_\xi{}^{(AT)}\}+$$
$$\lambda_a\overline{w}_{,\xi}+\lambda_d\overline{w}_{,\tau}+\lambda_c\int_0^1\int_0^1\overline{w}d\eta d\xi+\overline{w}_{,\tau\tau}-\frac{1}{\pi}\{$$
$$12\frac{a}{h}[\overline{u}_{,\xi}\overline{w}_{,\xi\xi}+\nu f^2\overline{u}_{,\xi}\overline{w}_{,\eta\eta}+(1-\nu)\,f^2\,\overline{u}_{,\eta}$$
$$\overline{w}_{,\xi\eta}+f^3\overline{v}_{,\eta}\overline{w}_{,\eta\eta}+\nu f\overline{v}_{,\eta}\overline{w}_{,\xi\xi}+(1-\nu)f\overline{v}_{,\xi}$$
$$\overline{w}_{,\xi\eta}]+6[\overline{w}^2_{,\xi}\overline{w}_{,\xi\xi}+f^4\overline{w}^2_{,\eta}\overline{w}_{,\eta\eta}+f^2\overline{w}^2_{,\eta}$$
$$\overline{w}_{,\xi\xi}+f^2\overline{w}^2_{,\xi}\overline{w}_{,\eta\eta}+f^2\overline{w}_{,\xi}\overline{w}_{,\eta}\overline{w}_{,\xi\eta}]\}=0 \qquad (1\text{-}c)$$

Where, $d_1=(1-\nu)/2$ and $d_2=(1+\nu)/2$

The form of these equations is general see Ref [1] and Ref. [9]. Galerkin's method is then used to reduce the obtained equations of motion to a set of nonlinear ordinary differential equations having the non-dimensional time variable as an independent variable. The displacement u, v, and the deflection w are expanded in the form of a generalized double series of modes. These modes satisfy the appropriate geometric boundary conditions of the plate, thus:

$$\overline{u}^o(\xi,\eta,\tau)=\sum_{m=1}^{\infty}\sum_{n=1}^{\infty}\overline{U}_{mn}(\tau)X^{(u)}{}_m(\xi)Y^{(u)}{}_n(\eta) \qquad (2\text{-}a)$$

$$\overline{v}^o(\xi,\eta,\tau)=\sum_{m=1}^{\infty}\sum_{n=1}^{\infty}\overline{V}_{mn}(\tau)X^{(v)}{}_m(\xi)Y^{(v)}{}_n(\eta) \qquad (2\text{-}b)$$

$$\overline{w}^o(\xi,\eta,\tau)=\sum_{m=1}^{\infty}\sum_{n=1}^{\infty}\overline{W}_{mn}(\tau)X^{(w)}{}_m(\xi)Y^{(w)}{}_n(\eta) \qquad (2\text{-}c)$$

where $X(\xi)$ and $Y(\eta)$ are the modal functions that satisfy the boundary conditions imposed on u, v, or w in the ξ and η direction respectively.

$$A1^{mn}_{ij}\overline{U}_{mn}+A2^{mn}_{ij}\overline{V}_{mn}+A3^{mnrs}_{ij}\overline{W}_{mn}\overline{W}_{rs}=0 \qquad (3\text{-}a)$$

$$B1^{mn}_{ij}\overline{V}_{mn}+B2^{mn}_{ij}\overline{U}_{mn}+B3^{mnrs}_{ij}\overline{W}_{mn}\overline{W}_{rs}=0 \qquad (3\text{-}b)$$

$$\overset{mn}{\underset{ij}{C1}}\ \overline{W}_{mn,_{\tau\tau}} + \lambda_d \overset{mn}{\underset{ij}{C1}}\ \overline{W}_{mn,_\tau} + \lambda_a \overset{mn}{\underset{ij}{C2}}\ \overline{W}_{mn} + \lambda_c \overset{mn}{\underset{ij}{C3}}\ \overline{W}_{mn} +$$

$$\overset{mn}{\underset{ij}{C4}}\ \overline{W}_{mn} \pm \{\ n_\xi^{(AL)} + n_\xi^{(AT)}\} \overset{mn}{\underset{ij}{C5}} \overline{W}_{mn} \pm \{n_\eta^{(AL)} +$$

$$n_\eta^{(AT)}\} \overset{mn}{\underset{ij}{C6}}\ \overline{W}_{mn} + \overset{mnlp}{\underset{ij}{C7}}\ \overline{U}_{mn} \overline{W}_{lp} +$$

$$\overset{mnlp}{\underset{ij}{C8}}\ \overline{V}_{mn} \overline{W}_{lp} + \overset{mnlprs}{\underset{ij}{C9}}\ \overline{W}_{mn} \overline{W}_{lp} \overline{W}_{rs} = 0 \qquad (3\text{-}c)$$

The vectors $\overline{U}_{mn}(\tau)$ and $\overline{V}_{mn}(\tau)$ are computed algebraically and substituted in the modal equation in its tensorial form to yield the Duffing-type equation in the following form:

$$\overset{mn}{\underset{ij}{C1}}\ \overline{W}_{mn,_{\tau\tau}} + \lambda_d \overset{mn}{\underset{ij}{C2}} \overline{W}_{mn,_{\tau\tau}ij} + \overset{mn}{\underset{}{C3}} \overline{W}_{mn} \pm \{n_\xi^{(AL)} + n_\xi^{(AT)}\}$$

$$\overset{mn}{\underset{ij}{C4}} \overline{W}_{mn} \pm \{n_\eta^{(AL)} + n_\eta^{(AT)}\} \overset{mn}{\underset{ij}{C5}}\ \overline{W}_{mn} + \lambda_a \overset{mn}{\underset{ij}{C6}}\ \overline{W}_{mn}$$

$$+ \lambda_c \overset{mn}{\underset{ij}{C7}}\ \overline{W}_{mn} - \overset{mnlprs}{\underset{ij}{T}}\ \overline{W}_{mn} \overline{W}_{lp} \overline{W}_{rs} = 0 \qquad (4)$$

This tensorial nonlinear ordinary differential equation represents a set of (ixj) nonlinear ordinary differential equation which can not be solved exactly.

To complete the solution, the boundary conditions for the plate must be specified. For the purpose of comparison with the result obtained by the experimental report by Ref. [10], the boundary conditions are specified to be clamped all around with no in-plane movements, so that the out of plane boundary condition is fully-clamped and the in-plane boundary condition is edge-fixed, and these conditions are written as:

$w = w_{,\xi} = u^\circ = v^\circ = 0$ at both x=0 & x=1   (5-a)

$w = w_{,\eta} = u^\circ = v^\circ = 0$ at both y=0 & y=1   (5-b)

And the modal functions are then given by: $X^{(u)}_m(\xi) = X^{(v)}_m(\xi) = \sin(m\pi\xi)$ (6-a)

And $Y^{(u)}_n(\eta) = Y^{(v)}_n(\eta) = \sin(n\pi\eta)$ (6-b)

While:

$X^{(w)}_m(\xi) = \cosh\alpha_m\xi - \cos\alpha_m\xi$
$\qquad -\gamma_m(\sinh\alpha_m\xi - \sin\alpha_m\xi)$ (6-c)

and: $Y^{(w)}_n(\eta) = \cosh\alpha_n\eta - \cos\alpha_n\eta$
$\qquad -\gamma_n(\sinh\alpha_n\eta - \sin\alpha_n\eta)$ (6-d)

where α_m and γ_m are the coefficients for the mth flexural mode and can be calculated from the following equation:

$\cosh\alpha_m\cos\alpha_m = 1$ (7-a)

$\cosh\alpha_m - \cos\alpha_m\xi - \gamma_m(\sinh\alpha_m$
$-\sin\dot\alpha_m) = 0$ (7-b)

The values of these coefficients are given in Table 1, see also Ref. [13] and [27]. Once the displacement modal functions are specified for the prescribed boundary conditions, the coefficients of integration represented by the matrices A1 to A3, B1 to B3, C1 to C9, and T can be calculated numerically, see Ref [13] and [27]. The number of the terms in the assumed displacement series solution given by (2-a), (2-b), and (2-c) are arbitrary.

Since an exact solution of equation (4) is not available, an approximate solution will be obtained by the method of harmonic balance. This method is used to seek a periodic solution. In the frequency domain the differential operator $d/d\tau$ is replaced by $j\omega$ and, consequently, the system of nonlinear differential equations is converted to a set of nonlinear algebraic equations. When this set has a solution with real positive values of frequency and amplitude and real values of the phase angles, it indicates the occurrence of limit-cycle oscillations of the specified form. Thus one seeks a solution of the following form:

$\overline{W}_{mn}(\tau) = A_{mn}\sin(\omega\tau + \Phi_{mn})$ (8-a)

$\overline{W}_{mn} = A_{mn}[\cos\Phi_{mn} + j\sin\Phi_{mn}]\sin\omega_\tau$ (8-b)

$\overline{W}_{mn,\tau} = \omega A_{mn}[j\cos\Phi_{mn} - \sin\Phi_{mn}]\sin\omega_\tau$ (8-c)

$\overline{W}_{mn,\tau\tau} = -\omega^2 A_{mn}[\cos\Phi_{mn} +$
$j\sin\Phi_{mn}]\sin\omega_\tau$ (8-d)

$\overline{W}_{mn}\overline{W}_{rs}\overline{W}_{pq} = A_{mn}A_{rs}A_{pq}\{[\cos\Phi_{mn}\cos\Phi_{rs}$

$\cos\Phi_{pq} - \sin\Phi_{mn}\sin\Phi_{rs}\cos\Phi_{pq} - \cos\Phi_{mn}$

$\sin\Phi_{rs}\sin\Phi_{pq} - \sin\Phi_{mn}\cos\Phi_{rs}\sin\Phi_{pq}] -$

$j[\sin\Phi_{mn}\sin\Phi_{rs}\sin\Phi_{pq} - \cos\Phi_{mn}\cos\Phi_{rs}$

$\sin\Phi_{pq} - \sin\Phi_{mn}\cos\Phi_{rs}\cos\Phi_{pq} - \cos\Phi_{mn}$

$\sin\Phi_{rs}\cos\Phi_{pq}]\}\sin^3\omega_\tau$ (8-e)

Where,
$$\sin^3\omega_r = \frac{1}{4}(3\sin\omega_r + \frac{3}{4}\sin3\omega_r) \qquad (8\text{-}f)$$
The second term which is of higher harmonic will be dropped out and:
$$\sin^3\omega_r = \frac{3}{4}\sin\omega_r \qquad (8\text{-}g)$$
Substituting $\overline{W}_{mn}$ from equations (8) into the Duffing type equation (4) and equating separately the real and imaginary parts of the equations, the set of 2(ixj) nonlinear algebraic equations in the unknown variables given by (ixj) amplitudes, ((ixj)-1) phase angles, and the flutter frequency (ω_f) is obtained. These equations are solved numerically by the modified Newton-Raphson algorithm.

III. Smart Structure System with Piezoelectric materials

The intelligent system consists of one or more microprocessors that analyze the responses from the sensors and use integrated control theory to command the actuators to apply localized strains/displacements to alter system response. A smart structure has the capability to respond to the external environmental changes (such as loads or shape change) as well as to the internal environment changes (such as damage or failure), see Ref. [20], [21], [24], and [25]. It incorporates the smart material actuators that allow the alteration of system characteristics (such as stiffness or damping) as well as of system response (such as strain or shape) in a controlled manner. In fact a smart structure involves four key elements: actuators, sensors, control strategies, and power conditioning electronics Fig. 8. Smart structures are basically classified into two main types which are, see Ref [20]:

- Passive smart structure: it contains a built in sensing device to continuously monitor the current state and serviceability of the structure. These allow us to have a clear view of how far away from failure a particular structure is.

- Active smart structure: it has embedded sensors to monitor and measure the performance of the structure, then it has the ability to compare the measured data with a certain specified values and has the means of control to perform the corrective action through an embedded actuators.

The piezoelectric effect relates mechanical effects to electrical effects. These effects are highly dependent upon their orientation to the poled axis. It is, therefore, essential to maintain a constant axis numbering scheme, see Fig. 2. All materials, regardless of their relative hardness, follow the fundamental law of elasticity. The elastic properties of the piezoelectric material control how well it will work in particular application. The relationship between stress and strain is Hooke's Law which can be expressed as:

$$\sigma = E\varepsilon \text{ or } \varepsilon = S\sigma \quad \text{for isotropic}$$
materials where $S = 1/E$ (9)
$$\sigma_i = E_{ij}\varepsilon_j \text{ or } \varepsilon_i = S_{ij}\sigma_j \text{ for } \text{anisotropic}$$
materials (10)

Fortunately, many of the constants in the formulas above are equal to zero for PZT piezoelectric ceramics. The non-zero constants are,

S_{11}, S_{22}, S_{33}, S_{12}, S_{13}, S_{23}, S_{44}, and S_{66} with $S_{11} = S_{22}$ and $S_{66} = 2 (S_{11} + S_{12})$

$$[S] = \begin{bmatrix} S_{11} & S_{12} & S_{13} & 0 & 0 & 0 \\ 0 & S_{22} & S_{23} & 0 & 0 & 0 \\ 0 & 0 & S_{33} & 0 & 0 & 0 \\ 0 & 0 & 0 & S_{44} & 0 & 0 \\ 0 & 0 & 0 & 0 & 0 & 0 \\ 0 & 0 & 0 & 0 & 0 & S_{66} \end{bmatrix} \qquad (11)$$

$$k^2 = \frac{\text{M. E. Converted to E. Charge}}{\text{M. E. Input}}$$
$$\text{or} = \frac{\text{E. E. Converted to M. Disp.}}{\text{E. E. Input}} \qquad (12)$$

IV. Flutter Control Using Smart Structure

The control system consists of distributed sensors and actuators

attached to or integrated with the plate to such a degree that the distinction between control functionality and structure functionality is blurred, see Ref. [12], [23], and [25]. The main important aspect in developing the active structure is the optimum choice of the materials and devices that can induce strains within the structure see Ref. [21], [22], and [26]. One of the materials that can produce forces and strains in the structure is the piezoelectric material. When an electric field is applied, the piezoelectric effect can be made to respond to (or cause) mechanical deformation in many different modes, such as thickness expansion, transverse expansion, thickness shear, or face shear. The piezoelectric materials in general are anisotropic and their electrical and mechanical responses differ, depending upon the axis of applied electric field or axis of mechanical stress or strain. The axes of the piezoelectric material are identified by numerals as shown in Fig. 2, where 1 correspond to length, 2 to width, and 3 to thickness. Two subscripts are used, where the first number always identifies the axis of the applied electric field, While the second number refers to the axis of induced mechanical strain or applied stress. The polarization axis is always the thickness or the 3 axis. Mechanical stress or strain can take place in all three directions. When an electric field is applied to a film of piezoelectric material, the film dimensions change in the direction of all three axes under stress free conditions. The degree to which these dimensions change relative to the applied field depends on the d_{ij} constant. So, d_{ij} can be defined as the stress-free ratio of the developed strain to applied field. For example d_{31} represents strain developed along axis (1) due to field applied along axis (3).

IV.1 Plate with PVF Piezoelectric Film as Distributed Actuator

A piezoelectric film of poly-Vinylidene-Fluoride (PVF2) is used as spatially distributed actuators. The properties of this piezoelectric film were shown in Table 2. The plate with two layers of (PVF2) film bonded perfectly to its upper and lower surface is shown in Fig. 3. The film used is biaxially polarized during its manufacturing, i.e. the field imposed across its faces will result in a proportional strain along the spatial dimension. As a result of the applied control voltage, an internal strain will be induced in both the (PVF2) and the plate. This strain results in a net stress in each layer to produce spatially uniform in-plane tensile forces. These forces are functions of the applied electric field as well as the elasticity and the thickness ratios. The strain induced in the plate due to the applied field on the piezoelectric layer is determined from the compatibility conditions. At the interface the strain in the plate will be same as that for the piezoelectric layer. The strain induced due to applied electric field is calculated and found to be:

$$\varepsilon_x^{(AV)} = \frac{\alpha}{\alpha + \psi} \quad d_{31} \quad \frac{V}{h_2} \qquad (13\text{-a})$$

$$\varepsilon_y^{(AV)} = \frac{\alpha + \psi}{\alpha + \psi} \quad d_{32} \quad \frac{V}{h_2} \qquad (13\text{-b})$$

where: ψ is the measure of the relative mechanical ratio of the structure to the actuator and is given by:

$$\psi = \frac{E_1 \, h_1}{E_2 \, h_2} \qquad (13\text{-c})$$

and α is the plate equilibrium parameter.

When an electric field is applied across both piezoelectric layers in the direction of the arrows shown in Fig. 4, the plate will be in extension, and α will equal to 2. If the field is applied across one piezoelectric layer in the direction of the arrow and reversed on the second, the plate will be deformed in bending, and α will equal to 6. Thus it is to be concluded that the piezoelectric layers

will be more effective in exciting surface strain in bending than in extension.

IV.2 Mathematical Modeling of the Composite Plate

In order to establish the fundamental elastic coupling of the piezoelectric-plate system, the static models of the actuator coupled to the plate given by (12-a) and (12-b) is used. The strains displacements relations for the plate with the two piezoelectric layers are given by:

$$\varepsilon_x = u^o_{,x} + (1/2)w^2_{,x} - zw_{,xx} + \varepsilon_x^{(AV)} \qquad (14\text{-}a)$$
$$\varepsilon_y = v^o_{,y} + (1/2)w^2_{,y} - zw_{,yy} + \varepsilon_y^{(AV)} \qquad (14\text{-}b)$$
$$\varepsilon_{xy} = u^o_{,y} + v^o_{,x} + w_{,x}w_{,y} - 2w_{,xy} \qquad (14\text{-}c)$$

As in the classical plate theory, the stress resultants and couples are given as:

$$[N^{(T)}_x, N^{(T)}_y, N^{(T)}_{xy}] =$$

$$\sum_{K=1}^{3} \int [\sigma^{(k)}_x, \sigma^{(k)}_y, \sigma^{(k)}_{xy}] \, dz \qquad (15\text{-}a)$$

$$[M^{(T)}_x, M^{(T)}_y, M^{(T)}_{xy}] =$$

$$\sum_{K=1}^{3} \int [\sigma^{(k)}_x, \sigma^{(k)}_y, \sigma^{(k)}_{xy}] \, zdz \qquad (15\text{-}b)$$

where the stresses for the kth layer are related to its strain through the constitutive relations:

$$\sigma^{(k)}_x = \frac{E_{(k)}}{1 - v_{(k)}^2}(\varepsilon_x + v_{(k)} \varepsilon_y) \qquad (16\text{-}a)$$

$$\sigma^{(k)}_y = \frac{E_{(k)}}{1 - v_{(k)}^2}(\varepsilon_y + v_{(k)} \varepsilon_x) \qquad (16\text{-}b)$$

$$\sigma^{(k)}_{xy} = G_{(k)} \varepsilon_{xy} \qquad (16\text{-}c)$$

In performing the previous integrations, care must be taken to obtain the correct stiffnesses and piezoelectric layer forcing terms. The piezoelectric layers and the plate will contribute to the extensional, coupling, and bending stiffnesses of the system while only the piezoelectric layer will produce the forces and moments.

Substituting the strains given by equation 13 into stress strain relation 15 and the results into equation 14, we get the expression for the resultant stresses

and couples in the plate with the two upper and lower piezoelectric layer represented in terms of displacements beside the stresses due to piezoelectric strain, see Ref. [12]. If Poisson's ratio for the plate material and the piezoelectric layers are assumed to be the same, then the resultant stresses and couples take the form:

$$N_x^{(T)} = Q_1^{..} \frac{E_1 h_1}{1 - v^2} \{[(u^o_{,x} + (1/2) w^2_{,x}) + v (v^o_{,y} +$$
$$(1/2) w^2_{,y})] + [(\varepsilon_x^{(AV)} + v\varepsilon_y^{(AV)})]\} \qquad (17\text{-}a)$$

$$N_y^{(T)} = Q_1^{..} \frac{E_1 h_1}{1 - v^2} \{[(v^o_{,y} + (1/2)w^2_{,y}) + v(u^o_{,x} +$$
$$(1/2)w^2_{,x})] + [(\varepsilon_y^{(AV)} + v \varepsilon_x^{(AV)})]\} \qquad (17\text{-}b)$$

$$N_{xy}^{(T)} = Q_1^{..} G_1 h_1 \{u^o_{,y} + v^o_{,x} + w_{,x} w_{,y}\} \qquad (17\text{-}c)$$

$$M_x^{(T)} = -Q_2^{..} \frac{E_1 h_1^3}{12(1 - v^2)} \{w_{,xx} + v w_{,yy}\} \qquad (17\text{-}d)$$

$$M_y^{(T)} = -Q_2^{..} \frac{E_1 h_1^3}{12(1 - v^2)} \{w_{,yy} + v w_{,xx}\} \qquad (17\text{-}e)$$

$$M_{xy}^{(T)} = -Q_2^{..} \frac{G_1 h_1^3}{6} \{w_{,xy}\} \qquad (17\text{-}f)$$

Where:

$$Q_1^{..} = (1 + 2\frac{1}{\psi}) \qquad (18\text{-}a)$$

$$Q_2^{..} = \{1 + 2\frac{1}{\psi}[3 + 6\frac{h_2}{h_1} + 4\frac{h_2^2}{h_1^2}]\} \qquad (18\text{-}b)$$

$Q_1^{..}$ and $Q_2^{..}$ are the contribution to the membrane rigidity and the flexural rigidity of the plate, respectively, due to the piezoelectric layers.

To distinguish between the membrane in-plane forces due to deflection of the plate and the in-plane tensile forces due to applied control voltage, it is preferable to write equations (16-a) and (16-b) in the following form:

$$N_x^{(T)} = N_x + N_x^{(AV)} \qquad (19\text{-}a)$$
$$N_y^{(T)} = N_y + N_y^{(AV)} \qquad (19\text{-}b)$$

Where:

$$N_x^{(AV)} = Q_1^{..} \frac{E_1 h_1}{1 - v^2} \{\varepsilon_x^{(AV)} + v\varepsilon_y^{(AV)}\} \qquad (20\text{-}a)$$

$$N_y^{(AV)} = Q_1^{..} \frac{E_1 h_1}{1 - v^2} \{\varepsilon_y^{(AV)} + v\varepsilon_x^{(AV)}\} \qquad (20\text{-}b)$$

The obtained resultant stresses and couples are substituted into equation of equilibrium given in Ref. [13] and [27], to get the equations of motion of the plate with the piezoelectric layers. These equations are nondimensionalized using the same nondimensional parameters given before. The only terms which are not included in the previous equations are the voltage induced in-plane forces. These two terms are non-dimensionalized as follows:

$$\overline{n_\xi}^{(AV)} = -\frac{12\,a^2}{\pi^4\,h_1^2}\{1+\frac{2}{\psi}\}\{\frac{\alpha}{\alpha+\psi}\}$$

$$\{d_{31} + \upsilon\,d_{32}\}\,\frac{V}{h_2} \qquad (21\text{-a})$$

$$\overline{n_\eta}^{(AV)} = \frac{12\,a^2\,f^2}{\pi^4\,h_1^2}\{1+\frac{2}{\psi}\}\{\frac{\alpha}{\alpha+\psi}\}$$

$$\{d_{31} + \upsilon\,d_{32}\}\,\frac{V}{h_2} \qquad (21\text{-b})$$

and the w-equation will be:

$$\frac{1}{\pi^4}\{\overline{W}_{,\xi\xi\xi\xi}+2f^2\,\overline{W}_{,\xi\xi\eta\eta}+f^4\overline{W}_{,\eta\eta\eta\eta}\} - n_\xi^{(AV)}$$

$$\overline{W}_{,\xi\xi} - n_\eta^{(AV)}\overline{W}_{,\eta\eta} + \lambda_a\overline{W}_{,\xi} + \lambda_d\overline{W}_{,\tau} + \overline{W}_{,\tau\tau} -$$

$$\frac{1}{\pi^4}\{12\frac{a}{h}[\,\overline{u}_{,\xi}\,\overline{W}_{,\xi\xi} + \upsilon\,f^2\overline{u}_{,\xi}\,\overline{W}_{,\eta\eta}+($$

$$1-\upsilon)\,f^2\overline{u}_{,\eta}\,\overline{W}_{,\xi\eta} +f^3\,\overline{v}_{,\eta}\,\overline{W}_{,\eta\eta}+\upsilon f\overline{v}_{,\eta}\overline{W}_{,\xi\xi}+($$

$$1-\upsilon)f\overline{v}_{,\xi}\,\overline{W}_{,\xi\eta}] + 6\,[\,\overline{w^2}_{,\xi}\,\overline{W}_{,\xi\xi} + f^4\,\overline{w^2}_{,\eta}$$

$$\overline{W}_{,\eta\eta} + f^2\overline{w^2}_{,\eta}\,\overline{W}_{,\xi\xi}+f^2\,\overline{w^2}_{,\xi}\overline{W}_{,\eta\eta}+ f^2\,\overline{W}_{,\xi}$$

$$\overline{W}_{,\eta}\,\overline{W}_{,\xi\eta}\,]\} =0 \qquad (21\text{-c})$$

It is worthwhile to mention that the cavity term and the in-plane forces due to applied loads and thermal stresses terms are dropped out for the investigation of the effect of the piezoelectric actuators alone. The nondimensional equations are solved by the same procedures shown before. The final form of the equation represents the nondimensional deflection as function of both the aerodynamic loading and damping, and

the in-plane applied forces due to piezoelectric layers. Fig. 5 shows the flutter point for the same weight of the plate with and without piezoelectric materials, where the voltage applied is $V = 4.3 \times 10^5$ volts. It is clear from the figure that for this particular value of the applied control voltage V, the induced in-plane tensile forces affect the plate flutter by shifting its critical value to about twice the value for the plate without treatment. By increasing the value of the applied voltage the critical aerodynamic loading is shifted more and more toward higher values. The limiting of this process is the operating condition of the plate. In the field of aircraft and spacecraft, the use of high voltage is not recommended from point of view of safety consideration. To avoid the usage of a high voltage, it is necessary to investigate the factors affecting this high voltage. Piezoelectric layers have two distinct effects. Firstly, it increases the plate membrane and flexural rigidities, and secondly, the applied electric field will produce extra in-plane tensile forces. These forces are given in its nondimensional form by equation 20 and are functions of the controlled applied voltage V and the relative mechanical ratio ψ. In case when the modulus of elasticity and the thickness of these layers are small relative to that of the base plate (as the case of the PVFD2), the first effect is small and may be neglected. On the other hand, the second effect which depends mainly on the piezoelectric material properties beside its elasticity properties will be small and consequently high voltage will be required to do the task. The higher the values of the piezoelectric constants d_{31} and d_{32}, the modulus of elasticity E_2, and the thickness h_2, the higher the forces and the lower the required voltage.

IV.3 Plate with PZT Piezoelectric Ceramics as Distributed Actuator.

This previous observation encourages the seeking of some other materials with high piezoelectric constants and elasticity modulus. In fact, it is found that the mechanical and electrical properties of the PZT G-1195, PZT HST-41, or PZT G-1278 piezoelectric materials satisfy these requirements. They have higher values of both piezoelectric constants d_{ij} and the elasticity modulus. But on the other hand, they have higher densities and also they cannot be produced in the form of sheets like PVF2 film. It is found that using the properties of these materials in the previous formulations will decrease the required voltage dramatically. In other words, increasing the critical aerodynamic loading to the same values obtained by using PVF2 will require very low voltage compared to the previous case, which is acceptable from practical point of view. Fig. 6, shows the flutter point for the plate with and without piezoelectric material, where the voltage applied in this case is V = 80 volts. Fig. 7 shows a comparison between the plate with PVF2 and plate with PZT piezoelectric materials. It is clear from the figure that the PZT material is more effective.

V. Conclusion

The following conclusive statements can be summarized based on the investigations and results obtained.

-   For thin plates, where the deflection is at least of the same order of magnitude as the plate thickness, the nonlinear thin plate theory must be used. The nonlinearity, represented by the plate in-plane (membrane) forces created due to large deflection, is the main source that causes the amplitude of the plate deflection during flutter to be limited (limit cycle oscillation).

-   The accuracy of the result depends on the number of terms in the assumed series solution. For plates with high aspect ratio and when the direction of the flow is parallel to the longitudinal direction, the more terms in that direction, the more accurate the obtained results. It is found that using three terms in both directions gives good agreements with the experimental results.

-   In-plane applied tensile load has great stabilizing effect by suppressing flutter. These externally applied in-plane loads can be obtained thermally by assembling a pre-stressed plate or electrically by bonding two layers of piezoelectric materials to both the upper and lower surfaces of the plate. When a voltage is applied to these piezoelectric layers, an induced strain in the plate material takes place and consequently tensile in-plane load is obtained. These tensile loads shift the onset of flutter point to about twice the value of the critical dynamic pressure for the plate alone. The important factors that affect this technique are the electrical and mechanical properties of the piezoelectric material with respect to the plate material and the way the voltage is applied.

-   From these previous results, it is concluded that using the piezoelectric material is suitable for the prevention and control of flutter, without adversely affecting the weight and cost.

REFRENCES

[1] Bisplinghoff. R. L., Ashley, H., and Halfman, L. R. (1962). Aeroelasticity, Addison-Wesley Publishing Company, Inc.

[2] Dowell, E. H. (1975), Aeroelasticity of Plates and Shells, Noordhoff Int'l Publishing, pp. 51-70.

[3] Ashley, H. and Zartarian, G. (1956), "Piston Theory – A New Aerodynamic Tool for the Aeroelastician", Journal of Aeronautical Sciences, Vol. 23, pp. 1109-1118.

[4] Fung, Y. C. (1958), " On Two-Dimensional Panel Flutter", Journal of Aeronautical Sciences, Vol. 25, pp. 145-160.

[5] Dowell, E. H. and Voss, H. M. (1965), " Theoretical and Experimental Panel Flutter Studies in the Mach Number Range 1.0 to 5.0", AIAA Journal, Vol. 3, No. 12, pp. 2292-2304.

[6] Dowell, E. H. (1966), "Nonlinear Oscillations of a Fluttering Plate. I", AIAA Journal, Vol. 4, No. 7, pp. 1267-1275.

[7] Chia, C. Y. (1980), Nonlinear Analysis of Plates, McGraw Hill Int'l Book Company.

[8] Dowell, E. H. (1971), "Generalized Aerodynamic Forces on a Flexible Plate Undergoing Transient Motion in a Shear Flow with an Application to Panel Flutter", AIAA Journal, Vol. 9, No. 5, pp. 834-841.

[9] Timoshenko, S. and Woinowsky-Krieger, S. (1959), Theory of Plates and Shells, McGraw-Hill Book Company, Inc., N.Y.

[10] Kappus, H. P., Lemley, C. E., and Zimmerman, N. H. (1971), "An Experimental Investigation of High Amplitude Panel Flutter", National Aeronautics and Space Administration. (NACA CR- 1837) Washington, D. C. May 1971.

[11] Dugundji, J. (1966), "Theoretical Consideration of Panel Flutter at High Supersonic Mach Number", AIAA Journal, Vol. 4, No. 7, pp. 1257- 1266.

[12] Crawley, E. F. and de Luis, J. (1987), "Use of Piezoelectric Actuators as Elements of Intelligent Structures", AIAA Journal, Vol. 25, No. 10, pp. 1373-1385.

[13] Abou-Amer S. 1991. "Control of Panel Flutter at High Supersonic Speed", submitted in partial fulfillment of requirements for the degree of doctor of philosophy in Mechanical and Aerospace Engineering in the Graduate School of the Illinois Institute of Technology. Chicago, Illinois.

[14] Dowell, E. H. (1973), "Aerodynamic Boundary Effect on Flutter and Damping of Plate", J. AIRCRAFT, Vol. 10, No. 1. pp. 734-738.

[15] Lock, M. H. and Fung, Y. C. (1961), "Comparative Experimental and Theoretical Studies of Flutter of Flat Panels in a Low Supersonic Flow", AFOSR TN 670, Guggenheim Aero. Lab., Calif. Inst. Tech., Pasadena, Calif.

[16] Tawfik, M., Bin Duan, J. R., and Mei, C. "Suppression of Post-Buckling Deflection and Panel-Flutter Using Shape Memory Alloy", Aerospace Engineering Department. Old Dominion University, Norfolk, VA, 23529

[17] Ventres, C. S. and Dowell E. H. (1970), "Comparison of Theory and Experiment of Nonlinear Flutter of Loaded Plates", AIAA Journal, Vol. 8, No. 1, pp. 2022-2030.

[18] Voss, H. M. and Dowell, E. H. (1964), "Effect of Aerodynamic Damping on Flutter of Thin Panels", AIAA Journal, Vol. 2, No. 1, pp. 119-120.

[19] Abdel-Motagaly, K., Bin Duan, J. R., and Mei, C. (2003) "Active Control of Nonlinear Panel Flutter under Yawed Supersonic Flow", AIAA- 1514, 7-10 April 2003.

[20] Ingerjit Chopra. 2002. Review of State of Art of Smart Structures and Integrated System. AIAA Jurnal. Vol. 40, No. 11, November 2002.

[21] ANAND K. ASUNDI. Smart Structures Research at NTU. Nanyang Technological University. Singapore

[22] James R. Phillips. Sr.Member of Technical Staff. Piezoelectric Technology Primer.

[23] Wilkie, W.K., et al. Low-Cost Piezocomposite Actuator for Structural Control Applications. Proc. SPIE's 7th Annual International Symposium on Smart Structures and Materials, Newport Beach CA, March 5-9, 2000.

[24] Sirohi, J., and Chopra, I. Fundamental Understanding of Piezoelectric Strain sensors. Journal of Intelligent Material Systems and Structures, Vol.11, April 2000, pp.246-257.

[25] Wada, B. K.. (1989), "Adaptive Structures", Transaction of the ASME,

Journal of Applied Mechanics, AD. Vol. 15, pp. 1-34.

[26] Eggborn, T. 2003. Analytical Models to Predict Power Harvesting with Piezoelectric Materials. For completion of Master of Science in Mechanical Engineering, Virginia Polytechnic · Institute and State University.

[27] Abou-Amer, S. A., El Nomrossy, M. M., and Dahshan, A. M. 2007, "Nonlinear Panel Flutter Analysis at High Supersonic Speed". Mansoura Engineering Journal, Vol. 32, No. 2, June 2007.
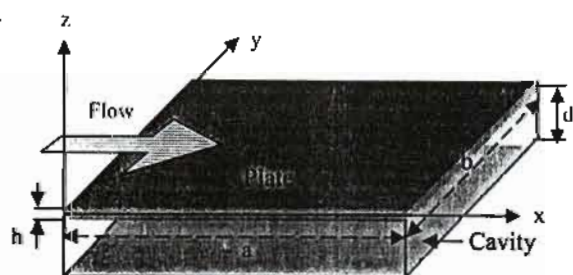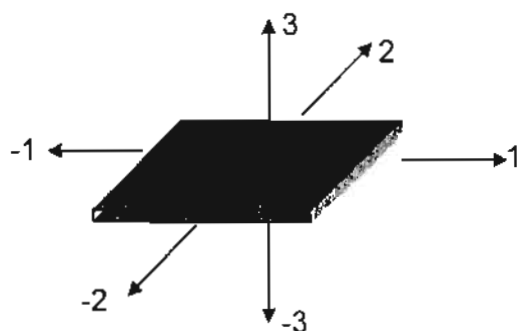
Fig. 1, Geometry of the Plate with Axes System

Fig. 2, Numerical Classification of the Axes of the Piezoelectric Film
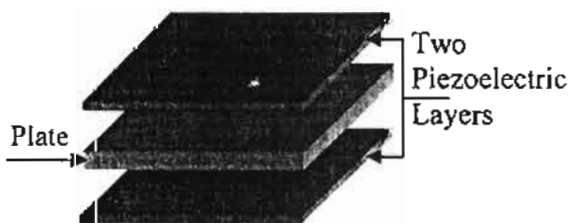
Fig. 3, Plate with Two Piezoelectric Layers at the Top and Bottom
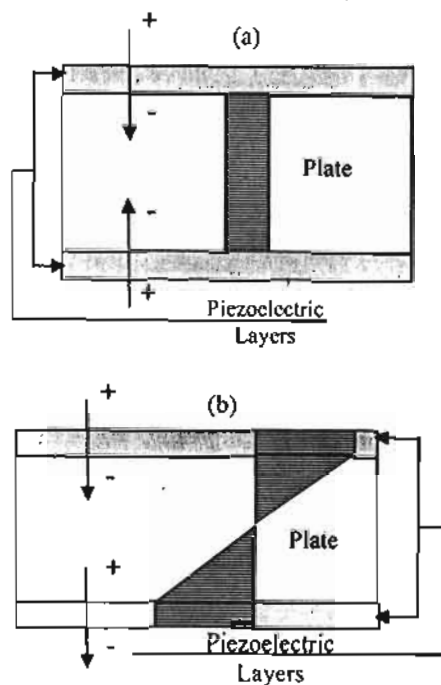
Fig. 4, Plate with Two Piezoelectric Layers Bonded Perfectly to its Upper and Lower Surfaces,
a) Extension, when the Applied Voltage are in the Same Direction.
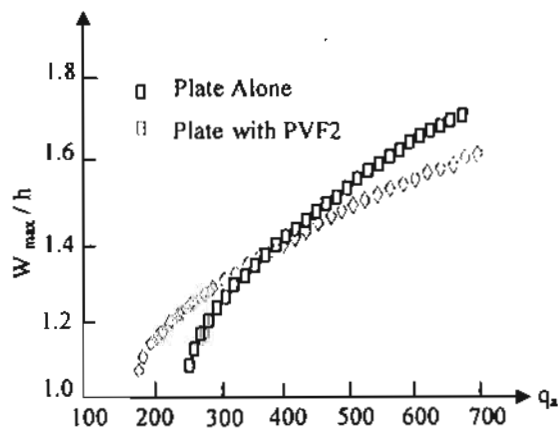b) Bending, when the Applied Voltage are in Opposite Directions.

Fig. 5, Flutter Characteristic of the Plate with and without PVF2 Piezoelectric Material (Applied Voltage is 43000 Volts)
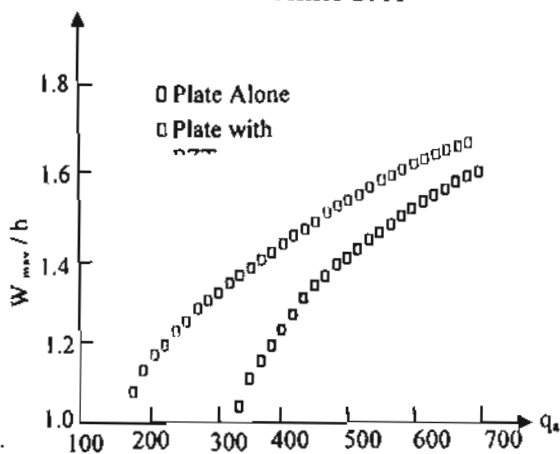
Fig. 6, Flutter Characteristic of the Plate with and without PZT Piezoelectric Material (Applied Voltage is 80 Volts)
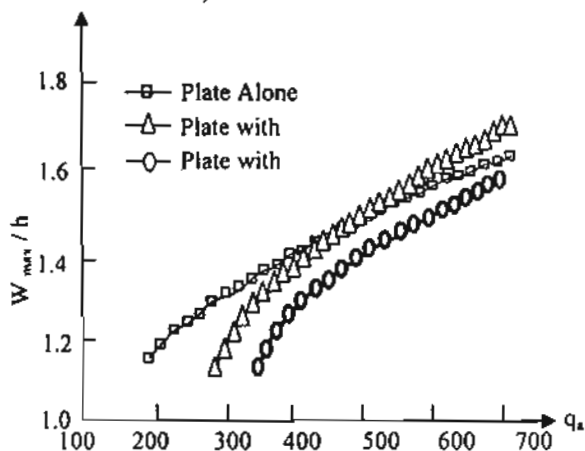

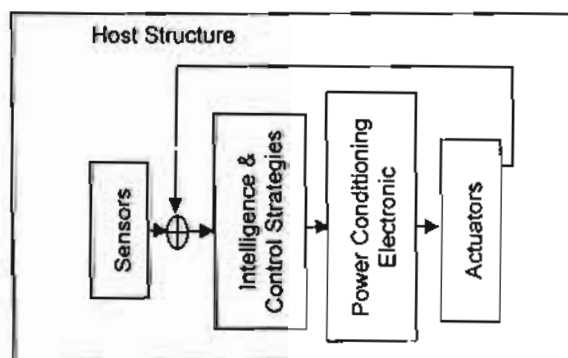Fig. 7, Comparison between the Plate, the Plate with PVF2, and the Plate with PZT Piezoelectric Materials

Fig. 8, Smart structure system with it's four basic key elements.

Table 1, Values of α_m and γ_m in the Beam Eigen function or a Clamped Plate.

M	α_m	γ_m
1	4.730040744862704 030	0.98250221457623 807
2	7.853204624095837 557	1.00077731190726 905
3	10.99560783800167 100	0.99996645012540 900
4	14.13716549125746 410	1.00000144989765 650
5	17.27875965739948 100	0.99999993734438 300
6	20.42035224562061 00	1.00000000270759 500
m > 6	$(2m+1)\pi/2$	1.0

Table 2, Dimensions and Properties of the Plate and the Treatment Piezoelectric Layers.

Dimensions and Properties	Plate	Piezoelectric Layer	
		PVDF 2	PZT
Availability		Sheet or Rolls	Segment
Length (m)	0.7620		38×10^{-3}
Width (m)	0.1778		15×10^{-3}
Thickness $(x10^{-3}m)$	0.8128	0.009 to 0.800	0.2500
Young's Modulus (x 10^9 N/m²)	72.398	2.0000	63.000
Shear Modulus (x 10^9 N/m²)	27×10^5		
Poisson's Ratio	0.3300	0.3300	0.3300
Density (x 10^3 kg/m³)	1.6189	1.8000	7.5000
Coefficient of Thermal Conductivity (μm/m.k)	11.700		
Loss Factor	0.0050		
Piezoelectric Strain Constant (x 10^{-12} V/m)		d_{31} =23 d_{32} = 3	d_{31} =190 d_{32} = 27